

## Synthesis and Characterization of Silicate Polymers

Simonsen, Morten Enggrob; Sønderby, Camilla; Søgaard, Erik Gydesen

*Published in:*  
Journal of Sol-Gel Science and Technology

*DOI (link to publication from Publisher):*  
[10.1007/s10971-009-1907-4](https://doi.org/10.1007/s10971-009-1907-4)

*Publication date:*  
2009

*Document Version*  
Accepted author manuscript, peer reviewed version

[Link to publication from Aalborg University](#)

*Citation for published version (APA):*  
Simonsen, M. E., Sønderby, C., & Søgaard, E. G. (2009). Synthesis and Characterization of Silicate Polymers. *Journal of Sol-Gel Science and Technology*, 50(3), 372-382. <https://doi.org/10.1007/s10971-009-1907-4>

### General rights

Copyright and moral rights for the publications made accessible in the public portal are retained by the authors and/or other copyright owners and it is a condition of accessing publications that users recognise and abide by the legal requirements associated with these rights.

- Users may download and print one copy of any publication from the public portal for the purpose of private study or research.
- You may not further distribute the material or use it for any profit-making activity or commercial gain
- You may freely distribute the URL identifying the publication in the public portal -

### Take down policy

If you believe that this document breaches copyright please contact us at [vbn@aub.aau.dk](mailto:vbn@aub.aau.dk) providing details, and we will remove access to the work immediately and investigate your claim.

# Synthesis and characterization of silicate polymers

Morten E. Simonsen · Camilla Sønderby ·  
Erik G. Søgaard

Received: 5 September 2008 / Accepted: 21 January 2009 / Published online: 12 February 2009  
© Springer Science+Business Media, LLC 2009

**Abstract** In this work an inorganic polymer is developed based on Elkem microsilica and potassium hydroxide. Using experimental data and the partial charge model a model for the gelation is suggested based on the hydrolysis and condensation reactions occurring during synthesis. In addition the optimal composition of the binder system was determined using compressive strength test and solubility experiments. Based on partial charge calculations and experimental data for the hydroxide concentration and the viscosity obtained in this study it is suggested that the polymerization of the inorganic polymer is determined by the concentration of silica species. It was found that the alkalinity has a crucial effect on the condensation process. The optimal potassium hydroxide concentration used in the synthesis of the inorganic polymer was found to be around 3.5 M, which resulted in a compressive strength of the product in the region of 50 MPa.

**Keywords** Sol–gel process · Inorganic polymer · Amorphous silica

## 1 Introduction

The development of inorganic polymers is a new promising technology that may be used in many applications. The synthesis of inorganic polymers is normally carried out by mixing an amorphous material for example silicium dioxide with a mineral base.

In previous work amorphous silica (fumed silica, microsilica) has been used as one of the reactive components in the preparation of Geopolymers usually in combination with an alumina source in the form of fly ash or metakaoline [1–5]. The addition of amorphous silica in Geopolymer synthesis resulting in an increase in the Si/Al ratio has been found to increase the strength of the binder [3, 4]. Moreover microsilica is routinely used as an additive in high performance cement. The addition of microsilica to Portland cement accelerates the hydration and formation of C<sub>3</sub>S. In the hydration process microsilica is consumed and an increased amount of calcium silicate hydrates are formed [6].

The reaction of silicate or aluminosilicate with a highly concentrated alkali solution or silicate solution can produce inorganic polymers with properties similar to Portland cement depending upon the composition and curing technique [7]. Variation in the preparation conditions of the inorganic polymers can result in a wide variety of properties, including high compressive strength, fire resistance and low thermal conductivity [7, 8]. These advantages make inorganic polymers a promising technology for new construction materials even though the cost for manufacturing Portland cement is relatively low (0.05–0.08 USD/kg, year 2006) [7].

The synthesis of the inorganic polymer is a result of dissolution of the surface of the amorphous silica particles by hydroxide resulting in formation of soluble silica species in the solution. The silica species are assumed to polymerise through condensation reaction resulting in formation of oligomers (dimers, trimers). The size and number of oligomers in the system increase until they extent throughout the solution resulting in formation of a gel. After gelation the system continues to rearrange and reorganize resulting in a three-dimensional network [8].

---

M. E. Simonsen · C. Sønderby · E. G. Søgaard (✉)  
Section of Chemical Engineering, Esbjerg Institute  
of Technology, University of Aalborg, Niels Bohrs vej 8,  
6700 Esbjerg, Denmark  
e-mail: egs@aaue.dk

Panagiotopoulou et al. [9] studied the dissolution of different industrial aluminosilicate minerals and by-products and reported that the extent of dissolution is higher when NaOH was used compared to KOH. It was suggested to be due to the smaller size of  $\text{Na}^+$  which better can stabilize the silicate monomers and dimers present in the solution, thus enhancing the minerals dissolution [10, 11]. The size of the cation is also reported to affect the morphology.  $\text{Na}^+$  displays strong ion-pair formation with smaller silicate oligomers, whereas  $\text{K}^+$  favors the formation of larger oligomers. As a result more polymer precursors exist providing better setting and stronger compressive strength when KOH is used compared to polymers synthesized in NaOH solutions [12]. In addition, the fact that  $\text{K}^+$  has a smaller hydration sphere radius than  $\text{Na}^+$  allows denser polycondensation reactions that increases the overall strength of the matrix [13].

In this work an inorganic polymer is developed based on amorphous silica (Microsilica 983 U, Elkem) and potassium hydroxide. Microsilica is an industrial by-product from the silicon production and is produced in great amounts around the world. Using experimental data and the partial charge model a model for the gelation is suggested based on the hydrolysis and condensation reactions occurring during synthesis. In addition the optimal composition of the binder system was determined using compressive strength test and solubility experiments.

## 2 Materials and methodology

The inorganic polymers were prepared by mixing 200 g amorphous silica (Microsilica) with 200 ml of a highly concentrated solution of potassium hydroxide in distilled water. The inorganic polymers were mixed for 10 h using a magnetic stirrer before casting in order to obtain homogeneous samples. In this work the molar concentration of potassium hydroxide was varied from 0.75 to 4 M. The microsilica used in the investigation is a by-product from the silicon production. Depending on the preparation method of silicon the microsilica vary in particle size and composition. The particle properties of different microsilica produced by Elkem are shown in

Table 1, when not specified otherwise the Elkem 983 U microsilica (Elkem 983 U) was used to prepare the inorganic polymers.

The pH of the solution was recorded during the synthesis using a special robust combi pH electrode (pHC2015-8) designed for alkaline samples. The evolution of the viscosity as a function of time was measured using a Brookfield model DV-III + programmable rheometer. The system was configured allowing mixing to take place between every viscosity measurement although not during the measurement.

Electro spray ionization mass spectroscopy (ESI-MS) analysis of the reaction solution was carried out using a LC-MSD-Trip-SL spectrometer from Agilent Technology. Samples for investigation were obtained during a reaction period of 24 h. The samples were prepared by centrifugation of 50 g of slurry for 10 min at 6000 rpm. The liquid part of the sample was filtrated using a 0.45  $\mu\text{m}$  filter and diluted 1:1000 in distilled water in order to avoid clogging of the capillary. The dry temperature was set at 325 °C and the dry gas was 5 L/min. The capillary exit voltage was 166 V. The solution was injected into the ESI-MS at a flow-rate of 0.3  $\mu\text{L}/\text{min}$ . The ESI-MS spectra of the inorganic silicate polymers were recorded in negative scanning mode in the spectral region 50–2200  $m/z$ .

The SEM images of the inorganic polymers were obtained using a LEO electron microscope 1500 with a GEMINI column.

Thermo Gravimetric investigation of the different inorganic polymers was carried out using a Mettler Toledo TGA/SDTA852e. The samples were prepared by placing 10 mg of the inorganic polymer in an aluminum oxide container and inserted into the instrument. The heat transfer rate used in the investigation was 10 °C/min and the applied temperature interval was 35–1000 °C.

The strength of the inorganic polymers was investigated using a compressive strength test. The test specimens for this test were cast in polypropylene containers with a diameter of 2.5 cm and a height of 5 cm. In order to avoid shrinking and cracks during drying 50 V/V% of quartz sand (0.1–0.3 mm) was added. The compressive strength test was performed on a Lloyd instrument LR 50 K, with a piston speed of 10 mm/min.

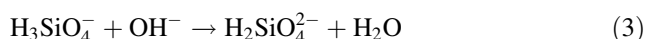
**Table 1** Particle properties and chemical composition of different Elkem microsilica

Chemical composition	Elkem 940 U	Elkem 983 U	Elkem 995 U
Loss by combustion	<3%	0.53%	Not tested
Silicium oxide ( $\text{SiO}_2$ )	>90%	98.6%	99.5%
Carbon	Not tested	0.24%	Not tested
BET	17.4 $\text{m}^2/\text{g}$	13.5 $\text{m}^2/\text{g}$	42.6 $\text{m}^2/\text{g}$
Particle radius (DLS)	159.2 $\pm$ 0.6 nm	198.5 $\pm$ 1.5 nm	127.7 $\pm$ 0.5 nm

### 3 Result and discussion

#### 3.1 Dissolution of silica particles

The synthesis of the inorganic polymers is thought to be a result of dissolution of the surface of the amorphous silica (Microsilica) particles by hydroxide resulting in formation of soluble silica species in the solution. The dissolution of the amorphous silica in alkaline conditions can be expressed by the following reactions.



These reactions suggest that  $\text{H}_2\text{O}$  and  $\text{OH}^-$  are consumed during the dissolution process resulting in a decrease in pH, which also was observed experimentally (Fig. 1). The solubility of amorphous silica is highly dependent on pH of the solution and a dramatic increase in the solubility is seen above pH 10 [14]. In addition, an increase in temperature will also increase the solubility of the amorphous silica. Dependent on pH different monomers will be present in the solution after dissolution ( $\text{H}_4\text{SiO}_4$ ,  $\text{H}_3\text{SiO}_4^-$ , and  $\text{H}_2\text{SiO}_4^{2-}$ ) [14]. It is the polymerization of these monomers that eventually lead to the formation of inorganic polymers.

In order to investigate the synthesis of inorganic polymers in greater detail pH of the solution was studied during synthesis. In Fig. 1 the pH evolution of the inorganic polymer synthesized from 0.75 to 4 M KOH are shown. From the figure it is seen that pH of the solution for the inorganic polymers synthesized using >1.5 M KOH is higher than 14 and thus above the normal measuring range

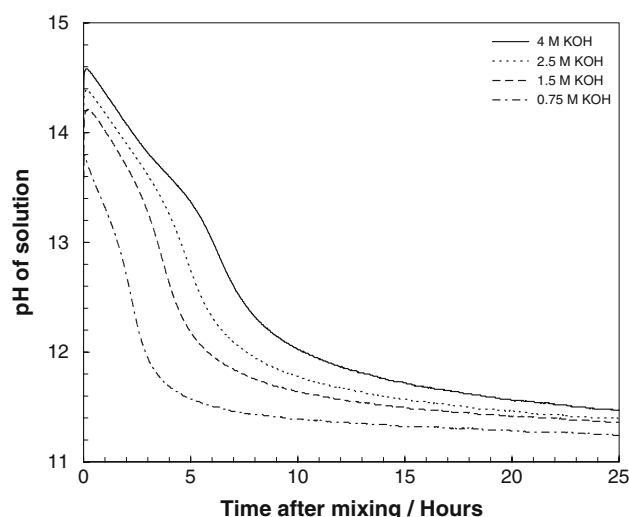
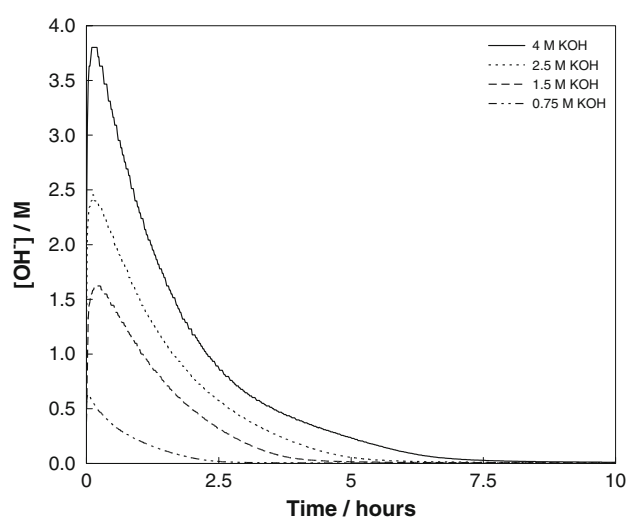


**Fig. 1** pH as a function of time after mixing for the inorganic polymer synthesized using 0.75–4 M KOH

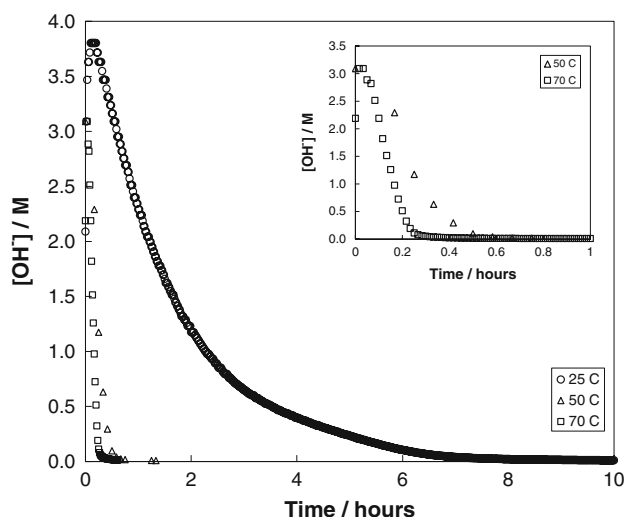
of the pH electrode (pH 14). However, repeating measurements of the pH evolution showed a good reproducibility and the measured hydroxide concentration agrees with the amount used in the synthesis, suggesting that the pH electrode in this case could be used to measure the pH evolution. In Fig. 2 the hydroxide concentration calculated from the pH measurements is shown as a function of the reaction time. The first part of the curves can be fitted to first order reaction kinetics. However, after a couple of hours of reaction the kinetics changes probably due to interference from products (dimers and oligomers) and the changes in the particle size of the microsilica due to dissolution. The accessibility of the microsilica surface is expected to be a limiting factor by inhibition effect from the resulting silicate species surrounding the particles. Moreover, it is seen that the dissolution proceeds for a longer time period when higher hydroxide concentrations are used resulting in higher dissolution. The increase in hydroxide concentration observed during the first 15 min can be ascribed to difficulties in pH measurements at high viscosity.

Figure 3 shows that an increase in the processing temperature has dramatically effect on the dissolution rate of the amorphous silica particles. An increase in the processing temperature of 25 °C resulted in a decrease in the reaction time from 10 h to about 30 min. Further investigations (Compressive strength test, XRD, and FT-IR analysis) have shown that although the temperature has a great influence on the rate of polymerization the properties of the final inorganic polymer do not change significantly.

Another parameter which is of importance during synthesis is the h ratio ( $m_{\text{H}_2\text{O}}/m_{\text{SiO}_2}$ ). An increase in water content will result in a decrease in the hydroxide concentration due to volume changes. Hence, the dissolution of



**Fig. 2** Hydroxide concentration as a function of the reaction time for different compositions of the inorganic polymers



**Fig. 3** Hydroxide concentration as a function of the reaction time for different processing temperatures of the inorganic polymer

silica will be lower thereby affecting the gel formation. Investigations showed that inorganic polymers synthesized using h ratio of 2 did not lead to gel formation.

### 3.2 Viscosity investigations

The viscosity development during the synthesis of the inorganic polymers was investigated during both the dissolution stage and the gelation stage as shown in Fig. 4. The viscosity increased rapidly during the initial mixing of microsilica and the hydroxide solution resulting in the development of a thick paste. After mixing the viscosity of the paste decreases as shown in Fig. 4. The decrease in

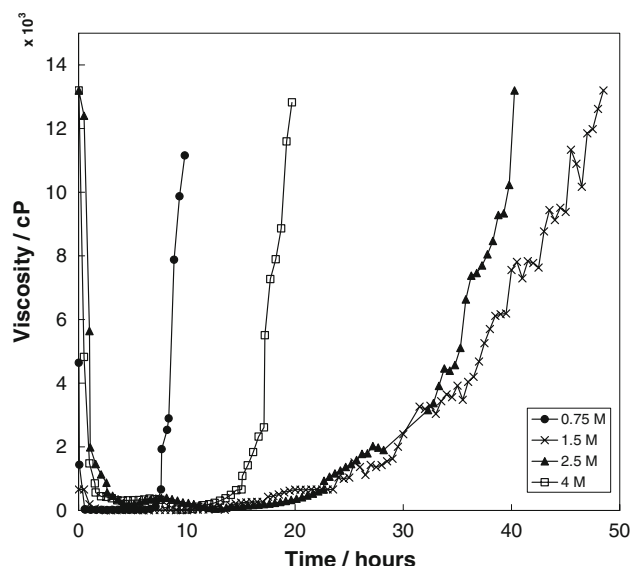


**Fig. 4** Measured viscosity of the inorganic polymer as a function of time after mixing

viscosity is thought to be due to two processes occurring during the initial dissolution step.

- Adsorption of  $\text{OH}^-$  ions on the surface of the silica particles resulting in negatively charged particles. As the solution consists of only negatively charged particles surrounded by positively charged cations the particles will be repelled by one another and hence the viscosity will decrease.
- Dissolution of the silica particles will cause the particles to decrease in size and number resulting in an additional decrease in viscosity.

The decrease in the viscosity is followed by a stable period in which virtually no change in the viscosity is observed. The duration of the stable period is dependent on the concentration of hydroxide used in the synthesis. Comparison with the measured evolution in hydroxide concentration during synthesis suggests that the dissolution process continues in the stable period. The stable period is followed by a significant increase in viscosity due to polymerization of the monomers or other initiating species leading to the extended network (gel) that results in formation of an inorganic polymer.

From Fig. 4 it is seen that the stable period with low viscosity is elongated if the hydroxide concentration is decreased from 4 to 1.5 M. This tendency has one exception, namely the lowest hydroxide concentration which has the shortest stable viscosity period. These results can be explained by two mechanisms occurring simultaneously. At high hydroxide concentration the surface of the silica particles will stay negatively charged during the dissolution process. As the concentration of silicate species in solution increase due to dissolution, polymerisation and later gel formation will occur. Higher concentrations of silicate species result in faster gel-formation. Hence, high hydroxide concentration results in fast gel-formation. That the 0.75 M hydroxide solution does not follow the general trend of faster gel formation with increasing concentration of hydroxide may be due to the fact that the amount of monomer produced is limited and that the hydroxide covered silica particles coagulate due to a lower surface charge destabilized by the presence of potassium ions.

The gel formation thus appears to be accelerated at high hydroxide concentrations and also at low hydroxide concentration resulting in a low surface charge density of the silica particles. A turn over point for these two mechanisms seems to be found with hydroxide concentrations between 0.75 and 1.5 M in the investigated systems.

### 3.3 Mass spectroscopy

As described above the dissolution of the amorphous silica particles is the first step in the synthesis of inorganic

polymers. The dissolution/hydrolysis process is followed by condensation reactions resulting in the formation of oligomers. This process releases the water that was initially consumed during dissolution. Thus, water only plays the role as reaction medium. The size and number of oligomers in the system will increase until they extend throughout the solution resulting in formation of a gel.

Electro spray ionisation mass spectrometry (ESI-MS) was used to identify the silicate species in the solution during polymerization. The assigned molecule ions were confirmed by the isotopic pattern of the elemental composition of the ion. All molecule ions were found as single negatively charged species, which were obtained by the removal of a proton ( $H^+$ ) from the molecule, thus leaving an anion that is subsequently detected.

From the ESI-MS spectrum shown in Fig. 5, it is seen that the most dominant peak is located at 155  $m/z$ , which can be assigned to a dehydroxylated dimer ( $Si_2O_3(OH)_3^-$ ). The second most intensive peak is assigned to a fully hydroxylated dimer ( $Si_2O_2(OH)_5^-$ ). Two monomeric species were identified in the mass spectra at 77 and 95  $m/z$  corresponding to  $SiO_2(OH)^-$  and  $SiO(OH)_3^-$  respectively. In addition a series of trimers are found at 233 and 271  $m/z$ . The most intensive of these trimers are found at 233  $m/z$  corresponding to a linear trimer with one oxo group or a cyclic trimer which usually is found in  $^{29}Si$  NMR investigations of silicate systems. It is not possible to distinguish between these two molecules using ESI-MS because this technique does not give information on the interconnectivity of the atoms in the molecule [15]. However, from these results it is observed that no high intensity peaks could be assigned to fully hydroxylated linear trimers ( $Si_3O_3(OR)_7^-$ ), suggesting that the trimers identified in this system under these conditions are present in the form of cyclic trimers. It should however be noted that Bussaian et al. have reported that the tendency of silica species not to appear as the fully hydroxylated ions increase with increasing silicate chain length [16].

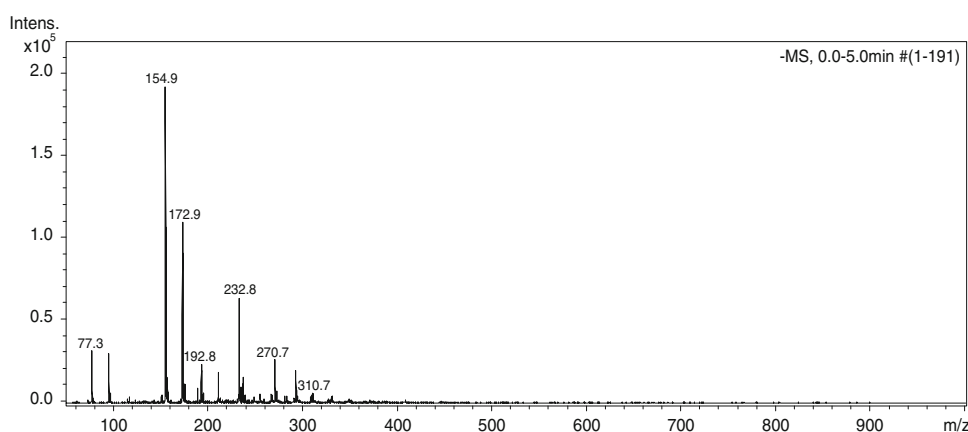
The peaks found at 293, 311, 331, 349, and 387  $m/z$  are assigned to dehydroxylated tetramers. However, the intensity of these peaks is below 10% of the most intensive peak. In addition pentamers and hexamers were also observed but again the intensity of these molecule ions was below 5%. The identified molecule ions in the mass spectra are listed in Table 2.

The evolution of the most dominant silicate species in the solution is shown in Fig. 6. From this figure it is shown that the intensity of the most dominant molecule ions increases up until 8 h after mixing. The increase of the intensity can be explained by the dissolution of microsilica leading to a greater amount of silicate species in the solution. The pH evolution during the dissolution process indicates that the dissolution process proceeds for approx. 10 h (Fig. 1) correlating with the observed

**Table 2** Silicate species identified in the reaction solution using ESI-MS

No.	$m/z$	Compound
1	77	$SiO_2(OH)^-$
2	95	$SiO(OH)_3^-$
3	155	$Si_2O_3(OH)_3^-$
4	173	$Si_2O_2(OH)_5^-$
5	193	$Si_2O_3(OK)(OH)_2^-$
6	211	$Si_2O_2(OK)(OH)_4^-$
7	233	$Si_3O_4(OH)_5^-$
8	271	$Si_3O_4(OK)(OH)_4^-$
9	293	$Si_4O_6(OH)_5^-$
10	311	$Si_4O_5(OH)_7^-$
11	331	$Si_4O_6(OK)(OH)_4^-$
12	349	$Si_4O_5(OK)(OH)_6^-$
13	371	$Si_5O_7(OH)_7^-$
14	387	$Si_4O_5(OK)_2(OH)_5^-$
15	447	$Si_5O_7(OK)_2(OH)_5^-$

**Fig. 5** ESI-MS spectra of an inorganic polymer synthesized using 4 M KOH 12 h after mixing





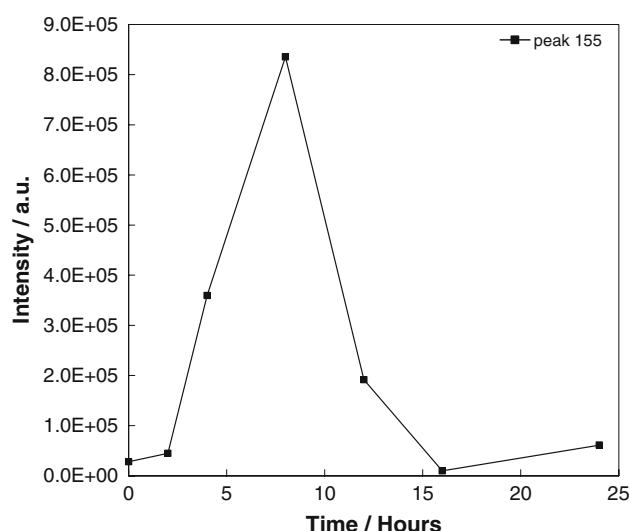


**Fig. 6** Intensity evolution of the most dominant peak in the ESI-MS spectra

increase in silicate species. The rapid drop in the intensity observed after 12 h in Fig. 6 is suggested to be due to polymerization of the soluble silica species. This is supported by the viscosity data in Fig. 4. From Fig. 4 it is seen that the viscosity of the inorganic polymers synthesized using 4 M KOH increases approximately 10 h after mixing, suggesting that polymerisation initiates at this point.

A broad band of low intensity signals were observed in the mass spectra after 12 h in the spectral region from 550 up to 1200  $m/z$ . These signals were found to consist of silicate species containing 6–12 Si atoms. If the polymerization occur by addition of monomers it would be expected to see a change in the mass spectra leading to peaks of relatively high intensity at higher  $m/z$  values. However, no such peaks were observed in the mass spectra. The change in the intensity of the most dominant silicate species in the mass spectra suggests that these species may serve as building blocks during the polymerization. It is believed that the polymerization lead to silicate species with  $m/z$  values greater than 2200 making detection no longer possible using the ESI-MS method. Another possibility is that the silicate species polymerize on the surface of the undissolved microsilica particles encapsulating the microsilica particles. During gelation the polymer encapsulated sphere of the microsilica particles may increase in size resulting in the formation of a network between the microsilica particles leading to gelation.

The presence of silicate species which serves as building blocks has also been proposed based on  $^{29}\text{Si}$  NMR investigation of the synthesis of zeosils and zeolites. In this case up to 20 different building blocks consisting were identified [15].

### 3.4 Partial charge model

In the following the step from initial condensation to a fully developed gel is discussed in greater detail by help of the partial charge model developed by Livage and coworkers [17]. Livage and coworkers have shown that the chemical reactivity of metal ions during the processes of hydrolysis and condensation can be predicted and explained by the partial charge distribution of the molecular species [17]. For instance, Weng and Sagoe-Crentsil [18] has applied the partial charge model to explain the hydrolysis and condensation reactions occurring during geopolymer synthesis [18–20].

Partial charge calculations for Si monomers in solution are shown in Table 3. The calculated  $\text{SiO}_2(\text{OH})_2^{2-}/\text{SiO}(\text{OH})_3^-$  ratio change from 2 to 0.2 in the pH range from 14 to 10, suggesting that the  $\text{SiO}_2(\text{OH})_2^{2-}$  ions is transformed into  $\text{SiO}(\text{OH})_3^-$  ions at lower pH. The  $\text{pK}_a$  value for the  $\text{SiO}_2(\text{OH})_2^{2-}/\text{SiO}(\text{OH})_3^-$  ion pair has been reported to be in the interval 12.6–13.1 [21–23]. In comparison the calculated shift in the  $\text{SiO}_2(\text{OH})_2^{2-}/\text{SiO}(\text{OH})_3^-$  ratio using the PCM was observed at pH 12.6.

Caullet and Guth [24] has calculated the distribution of the ionised forms of  $\text{Si}(\text{OH})_4$  versus pH, and their results showed that  $\text{SiO}(\text{OH})_3^-$  is the dominant species around pH 11 based on the equilibrium constants of the charged silicate species of  $\text{Si}(\text{OH})_4$  and that  $\text{SiO}_2(\text{OH})_2^{2-}$  increase with increasing pH higher than 11 which is in good agreement with the present calculation.

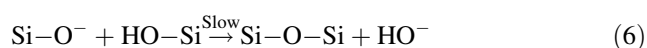
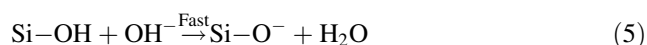
In the present work the pH of the slurry vary between ca. 14 to 11.5 during the cause of the reaction suggesting a shift in the  $\text{SiO}_2(\text{OH})_2^{2-}/\text{SiO}(\text{OH})_3^-$  ratio during the reaction. It was not possible to observe the  $\text{SiO}_2(\text{OH})_2^{2-}$  ion (47  $m/z$ ) in the mass spectra because the  $m/z$  value was below the detection range (50–2200  $m/z$ ).

According to the electronegativity equalization principle electron transfer stops when the electronegativities of all the atoms equal the mean electronegativity ( $\bar{\chi}$ ) which again is equal to the mean electronegativity of the solution [17]. Using the partial charge model (PCM) it was possible to calculate the silicate species which may be present at

**Table 3** Partial charge calculation for Si monomers in solution

pH	Partial charge of atoms			$\text{H}_2\text{SiO}_4^{2-}/\text{H}_3\text{SiO}_4^-$ ratio
	$\delta_{\text{O}}$	$\delta_{\text{H}}$	$\delta_{\text{Si}}$	
14	−0.47	0.02	0.18	2.0
13	−0.46	0.04	0.20	1.2
12.6	−0.46	0.05	0.21	1.0
12	−0.45	0.06	0.22	0.7
11	−0.43	0.07	0.24	0.4
10	−0.42	0.08	0.26	0.2

different pH. The calculated silicate species containing up to 5 Si atoms present at pH 14 and pH 10–12 are shown in Table 4. From the table it is seen that the silicate species at pH 14 have a charge higher than  $-1$  per Si atom in the molecule compared to the silicate species at pH 10–12 which have a charge of  $-1$  per Si atom. In addition the average partial charges of the different atoms in the silicate species are shown. Under the alkaline reaction conditions the polymerization will proceed through nucleophilic substitution reactions. In the nucleophilic substitution reaction between two silicate species the deprotonated oxygen ( $O^-$ ) on silicon will act as the nucleophile and the hydroxyl group as the leaving group as shown in the reaction scheme below.



From Table 4 it is seen that polymerization at high pH (pH 14) may not be favoured since the partial charge of the leaving group and the partial charge of the nucleophile are similar in size. In addition high degree of ionization of the silicate species at high pH results in repulsive interaction between the reactants hindering polymerization. Thus the monomeric, dimeric and trimeric species may be dominant at very high alkalinity. As the pH drop to below 12 the silicate monomers shift toward  $SiO(OH)_3^-$  and the mean electronegativity of the solution decrease. As a consequence the condensation between silicate species becomes more favourably. From Table 4 it is observed that the difference between the partial charge of the leaving group and the nucleophile is higher and the partial charge of the Si atom increase as a function of decreasing pH. In addition

the overall charge of the silicate species decreases resulting in less repulsion between the reactants. Thus, it is believed that the polymerization of the silicate species in the solution is determined by the alkalinity.

All the molecule ions identified in the reaction solution using ESI-MS were found as single charged molecules. However, partial charge calculation has shown that the charge of silicate species at pH 10–12 is in the order of  $-1$  per silicon atom in the molecule, suggesting that dimers have a negative charge of 2. It is possible that the ESI-MS technique may change the charge of the silicon species. Due to the very high ionic potentials of the nano sized aerosols in the spray electrons may be transferred to the high voltage positive electrode. As a consequence the charge of the silicate species determined by ESI-MS may not represent exactly the properties of the solution under examination prior to the mass analysis [25].

### 3.5 SEM analysis

SEM images of the inorganic polymers shown in Fig. 7 support the described dissolution/gelation model as a significant change in the particle size of the silica particles is observed when different concentrations of hydroxide was used. The SEM images also show that the amount of polymer/binder between the amorphous silica particles increases resulting in a higher density of the material as a result of higher hydroxide concentration used in the synthesis. The undissolved particles remain tied in the matrix, so that the strength and hardness of the microsilica particles correlates with the final strength.

### 3.6 TGA

In Fig. 8 the thermo gravimetric analysis of the inorganic polymers are shown. It was found that the amorphous silica (blank) used in this work does not give off any mass by increasing temperature. The amorphous silica that was used in these investigations had a purity of 98.6% (Table 1). Beside small amounts of carbon some metals were present, mainly Al and Mg. From Fig. 8 it is seen that 1–2% of water was removed from the samples at temperatures up to 100 °C. At higher temperatures excess potassium hydroxide was given off up to a temperature of 500 °C. In vacuum KOH sublimated unchanged at 400 °C forming dimeric species [26]. Thus, by help of TGA it was possibly to determine the amounts of excess potassium hydroxide that was not consumed in the sol–gel process.

### 3.7 Compressive strength

Investigation has shown that drying of large samples consisting only of inorganic polymer resulted in formation of

**Table 4** Calculated partial charges of possible silicate species in the reaction solution

Species	$\delta_O$	$\delta_H$	$\delta_{Si}$	$\delta_{OH}$	m/z
<i>High pH (14)</i>					
$SiO_2(OH)_2^{2-}$	−0.55	0.00	0.20	−0.55	47
$Si_2O_4(OH)_3^{3-}$	−0.52	0.04	0.25	−0.47	57
$Si_3O_6(OH)_4^{4-}$	−0.50	0.06	0.27	−0.44	62
$Si_4O_8(OH)_5^{5-}$	−0.50	0.07	0.28	−0.43	65
$Si_5O_{10}(OH)_6^{6-}$	−0.49	0.08	0.28	−0.42	67
<i>pH 10–12</i>					
$SiO(OH)_3^-$	−0.44	0.14	0.35	−0.30	95
$Si_2O_3(OH)_4^{2-}$	−0.45	0.12	0.34	−0.33	86
$Si_3O_5(OH)_5^{3-}$	−0.46	0.12	0.33	−0.34	83
$Si_4O_7(OH)_6^{4-}$	−0.46	0.11	0.33	−0.35	82
$Si_5O_9(OH)_7^{5-}$	−0.46	0.11	0.32	−0.35	81
$Si_6O_{11}(OH)_8^{6-}$	−0.46	0.11	0.32	−0.35	80



**Fig. 7** SEM images of inorganic binder at different potassium hydroxide concentrations: **a** 0.75 M, **b** 1.5 M, **c** 2.5 M and **d** 4 M

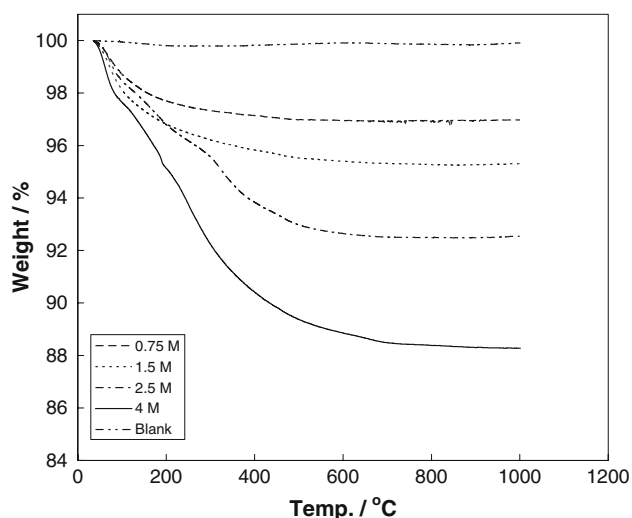
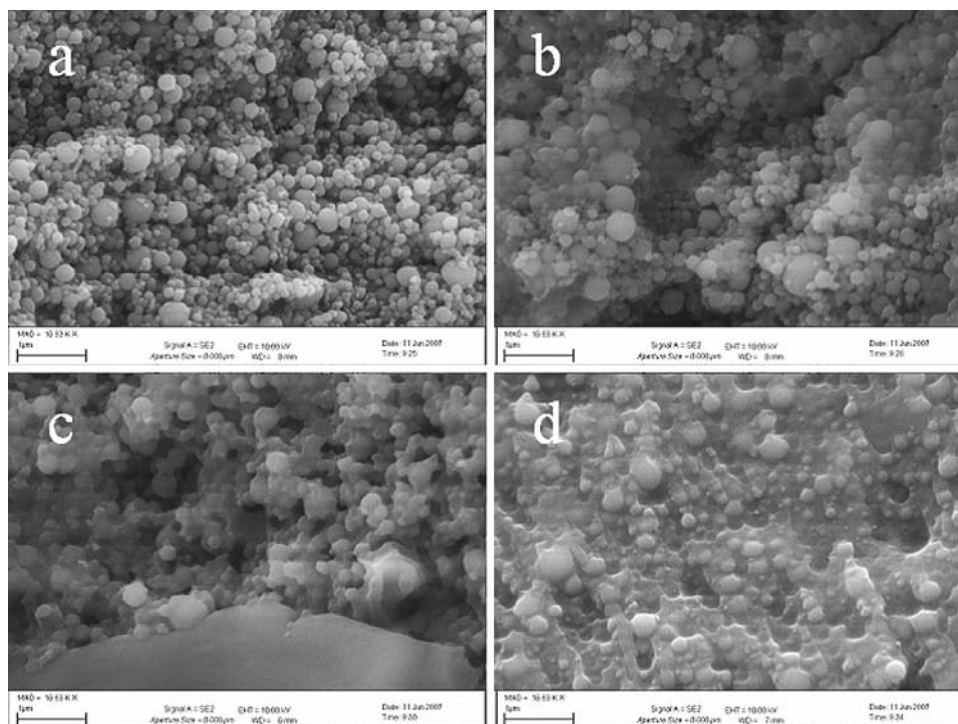


**Fig. 8** Thermo gravimetric analysis of the inorganic polymers synthesized using different potassium hydroxide concentrations

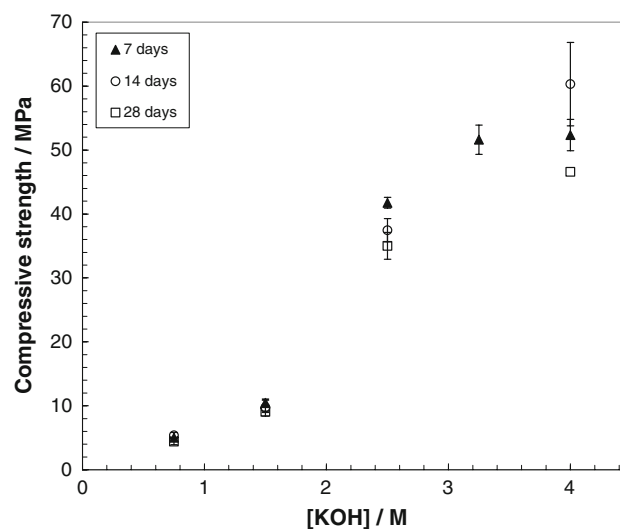


**Fig. 9** Compressive strength as a function of the potassium hydroxide concentration

cracks in the material. In the reported data for the compressive strength quartz sand was added in order to prevent the formation of cracks. The results of the compressive strength test showed that the strength of the inorganic polymer was strongly related to the concentration of potassium hydroxide used in the synthesis as shown in Fig. 9. The optimal potassium hydroxide concentration used in the synthesis of the inorganic polymer was found to be around 3.5 M, which resulted in a compressive strength in the region of 50 MPa. Furthermore, it is seen that the strength of the polymer is independent of the time after

synthesis (7, 14, 28 days). Similar compressive strength values have been obtained by Bajza et al. [27] for an inorganic binder synthesized using fumed silica, NaOH and  $\text{Na}_2\text{SiF}_6$ . In comparison fly ash based geopolymers synthesized from 10% metakaoline and 90% fly ash obtained a compressive strength of 35 MPa after 14 days [28]. Addition of up to 4% slag increased the compressive strength to 53 MPa which is comparable to the results obtained in the present work. However, the large variations in the fly ashes used in the synthesis of geopolymers influences the properties of the geopolymers ranging from

unworkable solutions to strengths of up to 95 MPa after 28 days [5].

In this work it was found that addition of glass fibers, iron, kaolin, and  $\text{TiO}_2$  particles increase the durability and strength of the material (data not shown). The addition of these materials reduces the strain in the material, and thus prevents the formation of cracks.

In order to investigate the strength development in greater detail the compressive strength was measured after 2 days up to 28 days as shown in Fig. 10. Figure 10 shows that inorganic polymers synthesized at 25 °C reach its final strength after 7–9 days. In comparison inorganic polymers synthesised at 50 °C obtain the final strength after only 4 days. The inorganic polymer synthesized at 70 °C did not reach a similar strength due to rapid evaporation of the water. Further investigation of the samples showed that the density of the inorganic polymers synthesized at 70 °C was much lower indicating higher porosity of the samples.

In Fig. 11 the significance of the density/porosity of the samples on the compressive strength are shown. The increase in density of the material is due to better adhesion between the inorganic polymer and the sand. The increase in adhesion can be ascribed to the increase in the amount of inorganic polymer formed at higher hydroxide concentration.

### 3.8 Chemical resistance

The chemical resistance of the developed inorganic polymers towards different test solution was investigated and the results are shown in Table 5. From the table it is seen that the inorganic polymer synthesized from the highest potassium hydroxide concentration (4 M) do not form a stable binder. However, it is shown that the inorganic

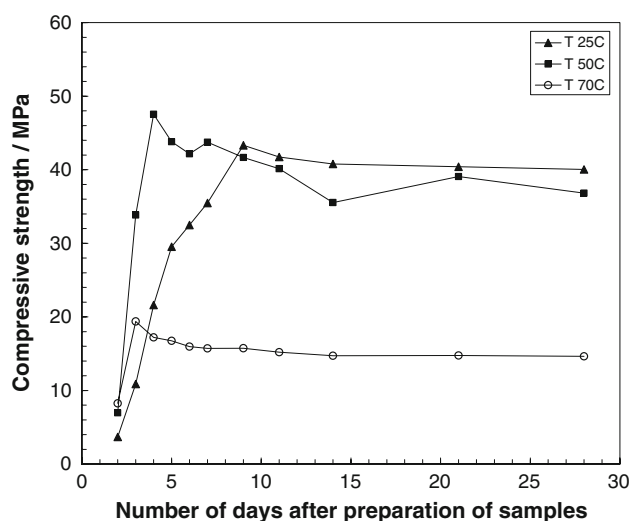


**Fig. 10** Strength development of the inorganic polymer during curing

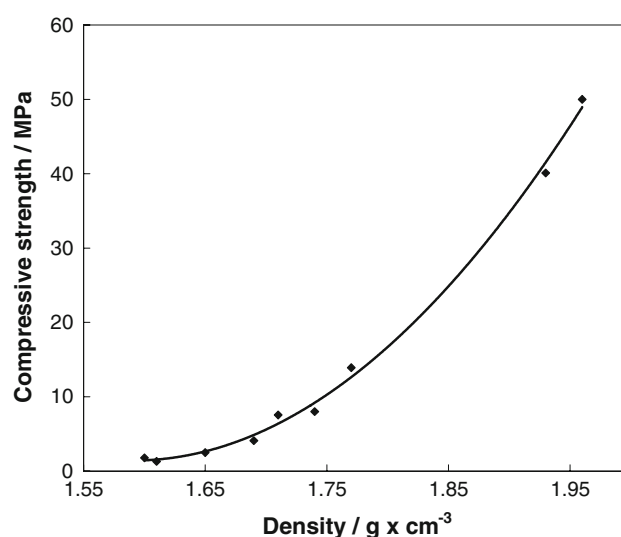


**Fig. 11** Compressive strength as a function of density of the inorganic polymers

**Table 5** Solubility experiments of the developed inorganic polymers

	0.75 M	1.5 M	2.5 M	4 M
Distilled water	ND	ND	ND	D
10 <sup>-5</sup> M NaCl	ND	ND	ND	D
10 <sup>-3</sup> M NaCl	ND	ND	ND	D
0.1 M NaCl	ND	ND	ND	D
10 <sup>-5</sup> M HCl	ND	ND	ND	D
10 <sup>-3</sup> M HCl	ND	ND	ND	PD
0.1 M HCl	ND	ND	ND	PD (gel formation)
10 <sup>-5</sup> M NaOH	ND	ND	ND	D
10 <sup>-3</sup> M NaOH	ND	ND	ND	D
0.1 M NaOH	D	D	D	D

In the table the solubility of the inorganic polymers is classified in three categories: Not dissolved (ND), Partly dissolved (PD), and Dissolved (D)

polymers suspended in acid show higher stability. It is believed that the acid neutralises excess hydroxide trapped in matrix of the inorganic polymer and thus stabilizes the inorganic polymer. In addition, it is seen that the inorganic polymers synthesized from  $\leq 2.5$  M hydroxide did not dissolve unless the inorganic polymers was suspended in 0.1 M NaOH in the present work.

In the synthesis of inorganic polymers many parameters influence the final properties. The time required for the inorganic polymer solution to form a continuous gel depends not only on the processing conditions but also the raw material (microsilica). The surface area of the particles which are dissolved has a great influence on the rate of dissolution and therefore on the gelation time of the inorganic polymer. The BET surface area provides an indication of how much surface area participates in the

heterogeneous reaction. Comparison between the gelation times for inorganic polymers synthesized using Elkem 995 (42.6 m<sup>2</sup>/g), Elkem 940 (17.4 m<sup>2</sup>/g), and Elkem 983 (13.5 m<sup>2</sup>/g) microsilica showed that the reaction of Elkem 995 microsilica (gelation time approximately 1.5 h) was significantly faster followed by Elkem 940 (gelation time approximately 15 h), Elkem 983 (gelation time 20 h). The gelation times of inorganic polymers synthesized from Elkem microsilica 940 and 983 varied considerably. The average particle size is higher for Elkem microsilica 983 resulting in the lowest BET surface area for the three described Elkem microsilica above. The small amounts of impurities which are present in the raw materials should also be taken seriously into account when modeling the gelation process.

#### 4 Conclusions

The synthesis of the inorganic binder is a result of dissolution of the surface of the amorphous silica (microsilica) particles by hydroxide resulting in formation of soluble silica species in the solution. In the developed physico-chemical model the silica species polymerise through a condensation reaction resulting in formation of oligomers. ESI-MS investigation of the reaction solution shows that monomers, dimers, and trimers are the most dominant species in the solution before polymerization. A drop in the intensity of these silicate species between 8 and 12 h after mixing was observed suggesting polymerization. It is believed that these species may be used as building blocks during polymerization. However, no high intensity peaks were observed at higher  $m/z$  values in the mass spectra after polymerization. Thus, the polymerization is believed to lead to silicate species with  $m/z$  values greater than 2200 making detection no longer possible using the ESI-MS method. Another explanation is that the silicate species polymerize on the surface of the undissolved microsilica particles leading to a polymer encapsulating microsilica particles. During gelation the polymer encapsulated microsilica particles increase in size resulting in the formation of a network between the microsilica particles.

SEM images of the inorganic polymers support the described dissolution/gelation model. Partial charge calculations showed that polymerization at high pH may not be favoured since the partial charge of the leaving group and the partial charge of the nucleophil is in the same order of magnitude. In addition high degree of ionization of the silicate species at high pH results in repulsive interaction between the reactants hindering polymerization. As the pH drop to below 12 the mean electronegativity of the solution decreases. As a consequence the condensation between silicate species becomes more favourably. It is suggested

that the polymerization of the silicate species in the solution is determined by the alkalinity.

The gelation of the inorganic polymers synthesized from different concentrations of KOH was studied by viscosity measurements. It was found that two mechanisms contributed to the time required for gelation. At high hydroxide concentration the high amount of silicate species in the system increase the rate of polymerization and therefore reduce the gelation time. At low hydroxide concentrations the surface charge of the silica particles is limited and the particles coagulate due to destabilisation by the presence of potassium ions. A turn over point for these two mechanisms seems to be found at hydroxide concentrations between 0.75 and 1.5 M in the investigated systems.

The optimal potassium hydroxide concentration used in the synthesis of the inorganic polymer was found to be about 3.5 M, which resulted in a compressive strength in the region of 50 MPa. In addition it was found that the inorganic polymers synthesized from  $\leq 2.5$  M hydroxide have good chemical resistance towards acid attacks and solutions with high ion strength.

The synthesis and final properties of inorganic polymers is highly influenced by the raw material (Microsilica). Comparison between the gelation times for inorganic polymers synthesized using Elkem 995, Elkem 940, and Elkem 983 microsilica suggested that the gelation time correlated with the surface area of the microsilica particles. In addition the content of impurities in the raw materials should also be taken into account.

#### References

1. Brew DRM, MacKenzie KJD (2007) *J Mater Sci* 42:3990. doi: [10.1007/s10853-006-0376-1](https://doi.org/10.1007/s10853-006-0376-1)
2. Zivica V (2004) *Bull Mater Sci* 27(2):179
3. Rowles M, O'Conner B (2003) *J Mater Chem* 13:1161. doi: [10.1039/b212629j](https://doi.org/10.1039/b212629j)
4. Fletcher RA, MacKenzie KJD, Nicholson CL, Shimada S (2005) *J Eur Ceram Soc* 25:1471. doi: [10.1016/j.jeurceramsoc.2004.06.001](https://doi.org/10.1016/j.jeurceramsoc.2004.06.001)
5. Davidovits J (2005) Geopolymer chemistry and sustainable development. In: Proceedings of the world congress geopolymer, Saint Quentin, France, Institut Géopolymère, Saint Quentin, 28 June–1 July 2005
6. Hjorth J, Skibsted J, Jacobsen HJ (1988) *Cem Concr Res* 18(5):789
7. Komnitas K, Zahataki D (2007) *Miner Eng* 20:1261. doi: [10.1016/j.mineng.2007.07.011](https://doi.org/10.1016/j.mineng.2007.07.011)
8. Duxson P, Fernández-Jiménez A, Provis J, Lukey G, Palomo A, Van Deventer J (2007) *J Mater Sci* 42:2917. doi: [10.1007/s10853-006-0637-z](https://doi.org/10.1007/s10853-006-0637-z)
9. Panagiotopoulou C, Kontori E, Perraki T, Kakali G (2007) *J Mater Sci* 42:2967. doi: [10.1007/s10853-006-0531-8](https://doi.org/10.1007/s10853-006-0531-8)
10. Xu H, Van Deventer J (2000) *Comput Chem* 24:391. doi: [10.1016/S0097-8485\(99\)00080-7](https://doi.org/10.1016/S0097-8485(99)00080-7)

11. Xu H, Van Deventer J (2003) *Colloids Surf A Physicochem Eng Aspects* 216(1–3):27. doi:[10.1016/S0927-7757\(02\)00499-5](https://doi.org/10.1016/S0927-7757(02)00499-5)
12. Phair J, Van Deventer J (2002) *Int J Miner Process* 66(1–4):121. doi:[10.1016/S0301-7516\(02\)00013-3](https://doi.org/10.1016/S0301-7516(02)00013-3)
13. Phair J, Van Deventer J (2001) *Miner Eng* 14(3):289. doi:[10.1016/S0892-6875\(01\)00002-4](https://doi.org/10.1016/S0892-6875(01)00002-4)
14. Iler RK (1979) *The chemistry of silica*. Wiley, New York
15. Eggers K, Eichner T, Woenckhaus J (2005) *J Mass Spectrom* 244:72. doi:[10.1016/j.ijms.2005.05.001](https://doi.org/10.1016/j.ijms.2005.05.001)
16. Bussian P, Sobott F, Brutschy B, Schrader W, Schüth F (2000) *Angew Chem Int Ed* 39(21):3901
17. Henry M, Jolivet J, Livage J (1992) *J Struct Bond* 77:153. doi:[10.1007/BFb0036968](https://doi.org/10.1007/BFb0036968)
18. Weng L, Sagoe-Crentsil K (2007) *J Mater Sci* 42:2997. doi:[10.1007/s10853-006-0820-2](https://doi.org/10.1007/s10853-006-0820-2)
19. Weng L et al (2005) *Mater Sci Eng B* 117:163. doi:[10.1016/j.mseb.2004.11.008](https://doi.org/10.1016/j.mseb.2004.11.008)
20. Weng L, Sagoe-Crentsil K (2007) *J Mater Sci* 42:3007. doi:[10.1007/s10853-006-0820-2](https://doi.org/10.1007/s10853-006-0820-2)
21. Langmuir D (1997) *Aqueous environmental geochemistry*. Prentice-Hall Inc., London
22. Brinker C, Scherer G (1990) *Sol-gel science, the physics and chemistry of sol-gel processing*. Academic Press, New York
23. Stumm W, Morgan J (1995) *Aquatic chemistry*, 3rd edn. Wiley, New York
24. Caullet P, Guth J (1989) *ACS Symp Ser* 398:83
25. Di Marco VB, Bombi GG, Tubaro M, Traldi P (2003) *Rapid Commun Mass Spectrom* 17:2039. doi:[10.1002/rcm.1147](https://doi.org/10.1002/rcm.1147)
26. Holleman AF, Wiberg E (1995) *Lehrbuch der Anorganischen Chemie*. Walter de Gruyter, Berlin
27. Bajza A, Rouseková I, Zivica V (1998) *Cem Concr Res* 28(1):13
28. Li Z, Liu S (2007) *J Mater Civ Eng* 19:470. doi:[10.1061/\(ASCE\)0899-1561\(2007\)19:6\(470\)](https://doi.org/10.1061/(ASCE)0899-1561(2007)19:6(470))